The Materials Research Society (MRS)
XXIII INTERNATIONAL MATERIALS RESEARCH CONGRESS 2014
NACE International Congress-Mexican Section

Javier Camarillo-Cisneros
Dirección. Centro de Investigación en Materiales Avanzados (CIMAV), Laboratorio Nacional de nanotecnología, Miguel de Cervantes No.120, C.P. 31109, Chihuahua, Chih., México
Tel: +52 (614) 152 0453
E-mail: javier.camarillo@cimav.edu.mx

Roberto Martínez-Sánchez*
Dirección. Centro de Investigación en Materiales Avanzados (CIMAV), Laboratorio Nacional de nanotecnología, Miguel de Cervantes No.120, C.P. 31109, Chihuahua, Chih., México
Tel: +52 (614) 439 1146
E-mail: Roberto.martinez@cimav.edu.mx

MICROSTRUCTURAL MODIFICATIONS ON 319 ALUMINUM ALLOY DUE TO CERIUM/LANTHANUM ADDITIONS

Abstract

Hardness and UTS measurements of commercial aluminum alloy 319 (AA319, Al-Cu-Si family) and Cerium/Lanthanum modified compositions were synthesized by casting process. The weight of Ce/La aggregates are in ranged from 0.25%/0.125% to 1%/0.5% wt. % Ce, respectively. For the as-cast stage, HR increased in all modified, while after solubilized and artificial-aging thermal treatments it was the UTS significantly enhanced, up to 20 MPa, both compared versus AA319 reference. Thermally treated samples and high temperature tests revealed superior UTS values to compositions containing Ce/La. The micrometric Ce/La precipitates interfere with fractures diffusion through the matrix, additionally due to their high thermal stability are not modified at the employed 250°C temperature. Rare earths additions allowed to increase the amount of Cu-θ' phase and reduced its dissolution rate at high temperatures.

Introduction

Strengthening of commercial aluminum alloys by means of nano phases precipitated after heat treatment is an active area in both technological and fundamental science. Its applications in automotive [1], aerospace and naval [2, 3] areas are due largely because possess an excellent weight/strength ratio [4, 5]. However, high temperature conditions, greater than 170° C, are a limiting factor since it decreases both mechanical properties in short periods of time. Cerium and/or Lanthanum [6, 7] additions to aluminum matrix have been considered as a promising alternative to increase hardness (HR) and ultimate tensile strength (UTS) at ambient [8] and high temperatures working conditions [9].

In this research we employed the commercial aluminum alloy 319 (AA319), containing as main alloying elements Al, Si and Cu. Microstructural modifications were related to Ce/La added fraction. Important changes was observed in in morphology of eutectic silicon and in the quantity of Al_2Cu (θ') phase. The time that the alloy remained the liquid state in the initial production process was an additional degree of freedom and its impact in mechanical properties is rationalized employing ultimate tensile strength. The employed synthesizing method is easily extensible to actual casting production in industrial scale.

Synthesis

The used materials include: AA319 and Al-6%Ce-3%La wt. % master alloy (ACL), both received in the form of ingots. The synthesis method comprises conventional casting; employing 2 kg of molten AA319 at 720°C in a graphite crucible and inside an electric furnace at ambient atmosphere. To reduce the harmful effect of dissolved hydrogen [10] it was degased the liquid alloy using Ar gas, introduced through a rotating graphite propeller for 5 min; longer degassing times does not significantly decrease the porosity. Ce/La modified versions were produced by direct addition of ACL into molten aluminum; referring the percentage of added Ce: 0.25, 0.5 and 1% wt. Ce (0.125, 0.25 and 0.50% wt. % La). As grain refiner it was employed Al-5Ti-B [11, 12] added in 0.33% wt. % before casting.

Finished products were subjected to T6 heat treatment consisted in: solubilized at 495°C for 5h, water quenching at 60°C, aged at 220°C for 3h and quenched into water at 25°C. The incipient thermal degradation was considered by maintaining T6 samples until 45 minutes at 250°C; work temperature (WT). To WT the hardness tests and tensile strength were measured after cooling the samples to room temperature. To UTS measurements under high temperature conditions (250°C, HT1), all samples were kept 45 min at the target temperature prior test.

Characterization

Microstructural analysis was performed employing scanning (SEM) and transmission (TEM) electron microscopies, SEM JEOL JSM-5800-LV, TEM Philips CM-200 and JEM-2200FS. Samples preparation were carried out by standard metallographic techniques, to SEM was employed 80% methanol-20% perchloric acid and to TEM were electro polishing with 70% methanol - 30% nitric acid at 20V and -30°C. E8-ASTM standard was followed to produce tension test specimens, tested in Instron-337 equipment at a speed of 0.1 mm/s. Regarding UTS conducted at high temperature, the furnace was maintained at 250°C for 2 h before testing. Hardness is reported in Rockwell B scale and measured in Wilson-Rockwell equipment. Chemical compositions are concentrated in Table I in atomic percent, obtained by inductively coupled plasma atomic emission spectroscopy (ICP-AES)).

Table 1. Chemical composition obtained by ICP-AES; AA319 and modified samples Ce/La.

	Ce	Si	Cu	Fe	Zn	Mg	Mn	Ti	Ni	Pb
AA319	-	7.941	2.51	0.703	0.391	0.331	0.256	0.120	0.039	0.019
+0.25%Ce	0.255	7.701	2.286	0.585	0.398	0.36	0.281	0.129	0.021	0.201
+0.5%Ce	0.506	7.457	2.095	0.577	0.366	0.335	0.256	0.117	0.018	0.017
+1%Ce	1.012	6.754	1.93	0.512	0.357	0.305	0.239	0.099	0.021	0.019

Results and Discussion

Microstructure

By means of SEM were observed Al dendrites; size, aspect ratio and morphologies in the matrix [13] were close similar, thus are characteristic independent of ACL composition. About the eutectic Si phases shown in Figure 1, the ACL addition had a clearly observable refinement effect, a very important characteristic to reduce fracture diffusion [14, 15]. The measurements corresponding to Si particles average area (Si_{av}) employed 10 fields at 200X per sample, representing around 11 000 μm^2. In the AC conditions (blue line) was obtained a decreased in Si_{av} to all Ce/La compositions; around 35% in the lower addition of 0.25% Ce (14 μm^2). Higher quantity in ACL, 0.5% Ce, had a small effect reducing Si_{av} to 11 μm^2. For 1% Ce the average area start to increase again, however remains markedly smaller in comparison to the unmodified AA319 sample. At T6 condition, the obtained values in Si_{av} (red line) correspond to a small difference respect to as-cast condition. It is qualitative appreciable the difference between Si spheroidization in the unmodified and 0.5Ce samples, showed in the insets of Figure 1. From blue and red lines comparison, can be concluded that the Si refinement is determined mostly for the initial casting conditions.

Even in the maximum reduction case, for the 0.25% Ce sample, it was around 2 μm^2 from AC to T6.

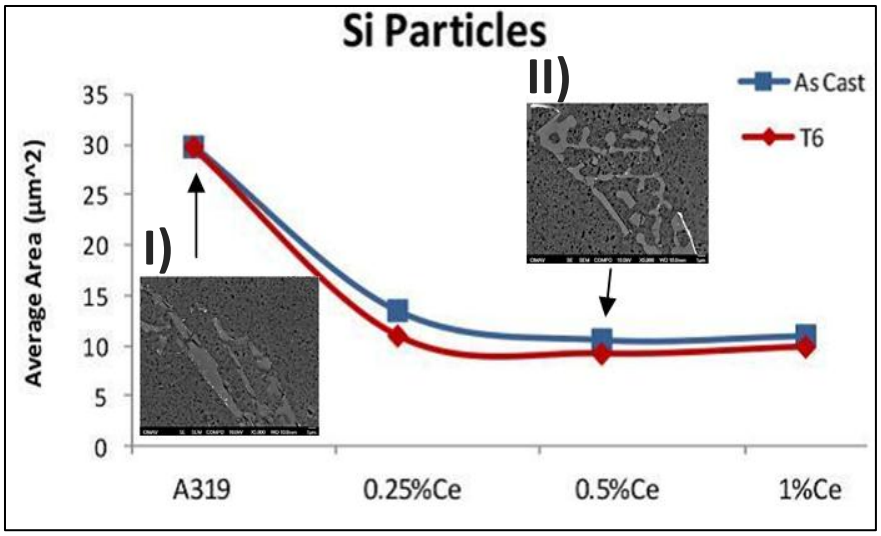

Figure 1: Eutectic Si average area, as-cast and T6 conditions are shown as function of Ce/La amount added. Insets correspond to SEM micrographs of eutectic Si: I) AA319 and II) 0.5% Ce.

ACL additions created needles with high fraction of Ce/La elements along the Al matrix (10.21Si, 0.95Fe, 0.91Ni, 23.85Cu, 4.4La, 7.51Ce, Al-bal); besides being related in small percent (<2% wt. %) to Cu-Si-Al phases to form a more complex inter metallic. Unlike eutectic Si precipitates, Ce/La needles remains practically with the same morphology and dimensions in all three modified compositions. Apparently the final needles are independent of the chemical composition employing low percent additions. A further feature is the time that the alloy spends in the liquid state (720°C) before being casting; this does not modified Ce/La precipitates, as is shown in Figure 2. However elemental composition obtained by EDS showed that Cu is slightly reduced in the matrix, around 2%.

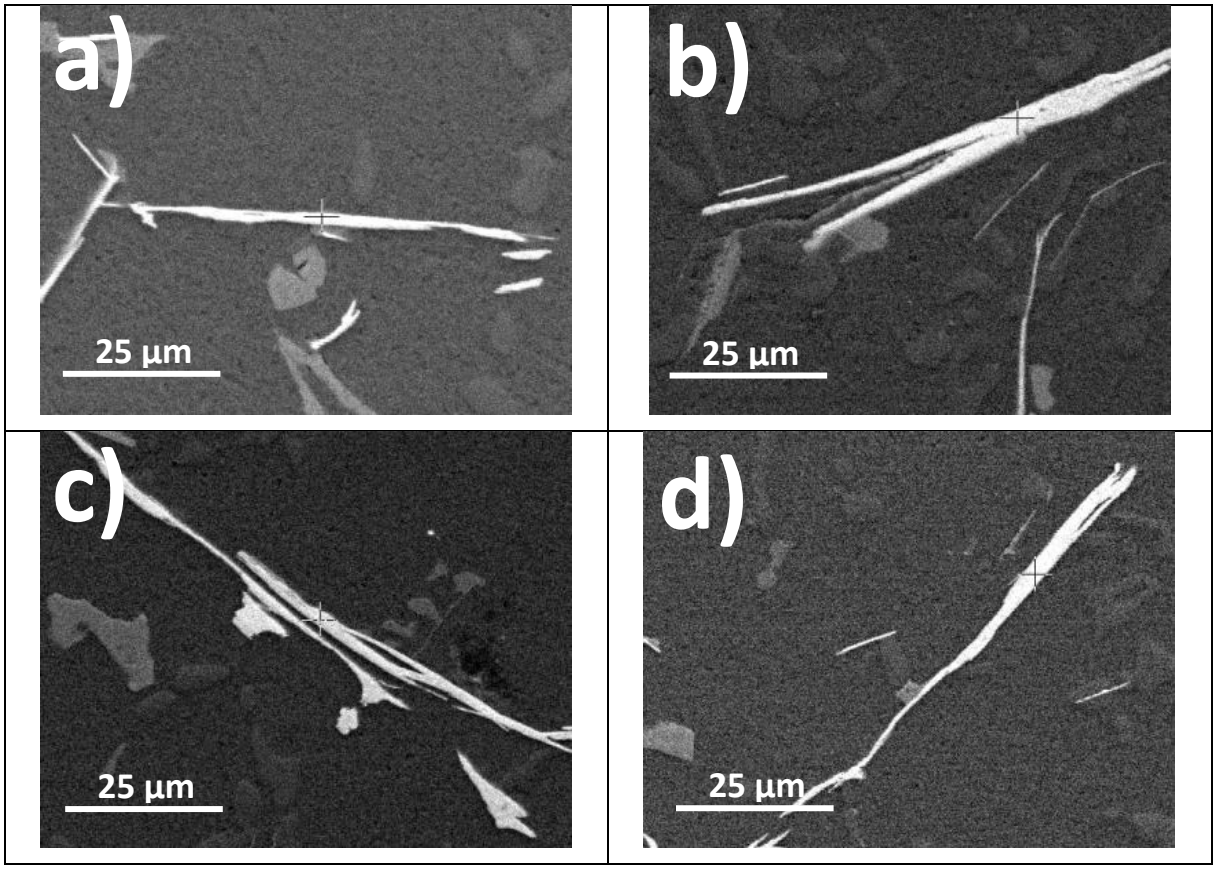

Figure 2. Ce-La needles function of time as the alloy stay in the liquid stage; a) 0 hrs, b) 1 hrs, c) 2 hrs y d) 3 hrs.

The effect of ACL additions over the known metastable θ' phases [16] was notorious, see micrographs in Z-contrast mode of Figure 3. Compared in T6 condition the quantity of θ' needles is similar in both AA319 reference and 0.5% Ce. Nevertheless, θ' pairs with a relative orientation of 90° between them are significantly higher in the modified composition. In case of WT, the Cu and Si precipitates were thickened. Significant changes were obtained in 0.5%Ce, is notorious the high quantity of θ' needles remaining with very close morphology respect its previous thermal state T6.

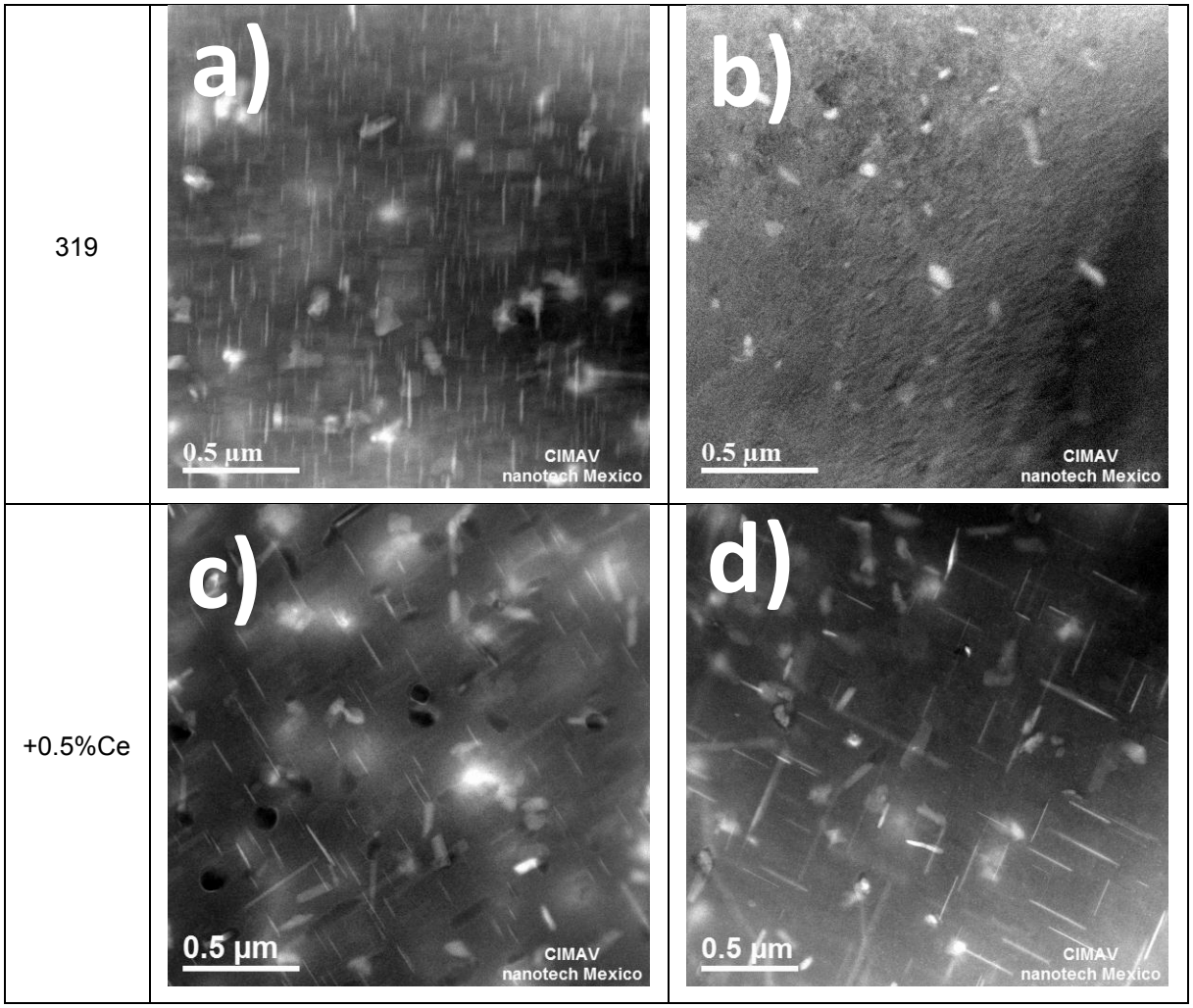

Figure 3. HR-STEM micrographs in Z contrast: a) AA319-T6, b) AA319-WT, c) 0.5Ce-T6, d) 0.5Ce-WT.

The interaction between Ce/La and θ' phase are shown by means of HR-STEM in Figure 4a. Can be observed θ' needles evenly distributed along the Al matrix, unexpectedly, these phases are limited or not available at all near to Ce/La needles. The Inset in Figure 4 a) shows an increased area of Ce/La needles in Z-contrast mode, the dark zones correspond to the lightest Al atoms. Due to the low amount of θ' phase near to Ce/La phases could be conclude that Cu diffusion has preference to Ce/La needles over two alternatives; remain dissolved in the matrix or to form θ' phases. However, It is also unclear whether once the θ' needles are formed the Cu may continue to diffuse to the Ce/La phases, times of 45 min at 250°C do not showed the existence of that process. Much longer averaging times, 100 hrs, does not dissolved completely Cu precipitates and does not thickened Al/Ce

phases. Previously we employed AA356 (Al-Si-Mg) alloy with Ce/La additions [17] incorporated by mechanical milling. In A356 the initial Ce/La particles with a size < 0.1 µm increased around the same dimensions of >50 µm as in the present work. Thus Cu diffusion to be incorporated into Ce/La needles should occur only at the T6 stage.

In Figure 4b) is shown an Al-Si-Cu precipitate after thickening [18, 19, 20, 21] due to WT condition, its size and morphology is representative of this time of phases founded with a wide range of stoichiometries. While micrograph it was obtained from the alloy AA319, these types of precipitates are presented on all employed compositions after overaging. Even after being thickened their orientation in a great percentage of them remains as in θ', parallel to the known [100] direction of the Al matrix, however now is coherent to the Al matrix, which is the reason for loss of mechanical properties.

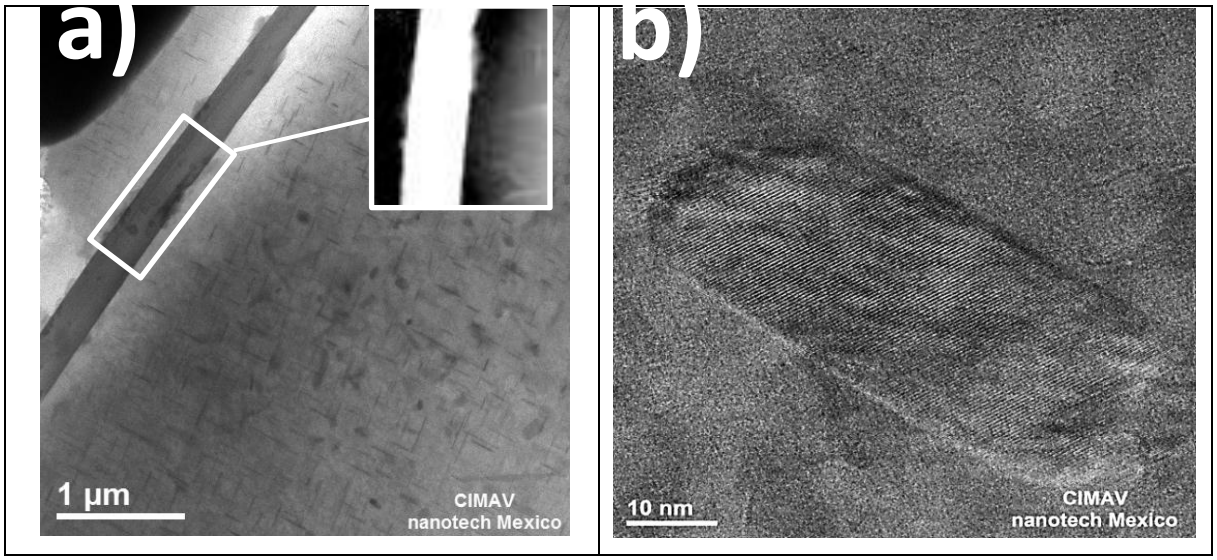

Figure 4. a) Ce/La needles, obtained from the modified composition 0.5% Ce, inset correspond to Z contrast mode. b) AA319 in WT condition.

Regarding mechanical properties, the values are concentrated in Figure 5 a) and b) respectively. Under operation conditions (T6 and WT), rare earth additions improved the response to both hardness and UTS. However, it is the production process, previous to casting, which is evaluated here, i.e. the influence of time over the alloy remaining in liquid stage had an influence in UTS; this is concentrated in Figure 5 c). Employing the 0.5% Ce modified composition, the liquid alloy was kept inside the container at 720°C synthesizing samples after 0, 1, 2 and 3 hours previous casting. The obtained values were fitted to a linear function, for the room temperature (blue line) and 250°C (red line) the tendencies were decrement in function of time. We related these decrement tendencies with EDS results obtained from Ce/La needles and matrix. Referring to 0 h condition (at

T6), the Cu content had a drop inside the matrix with an equal increase of Si element. Higher time in liquid state obtained higher quantity of Cu in the long ACL needles, thus we attribute the its matrix decrease by a diffusion to Ce/La needles. Nevertheless, it is not clear modifications done of Ce/La needles structures by Cu migration, almost by HR-STEM micrographs and EDS remain inside the same variations that an analysis of random needles in the matrix. To Si phase there was maintained the morphology unchanged by liquid phase residence time.

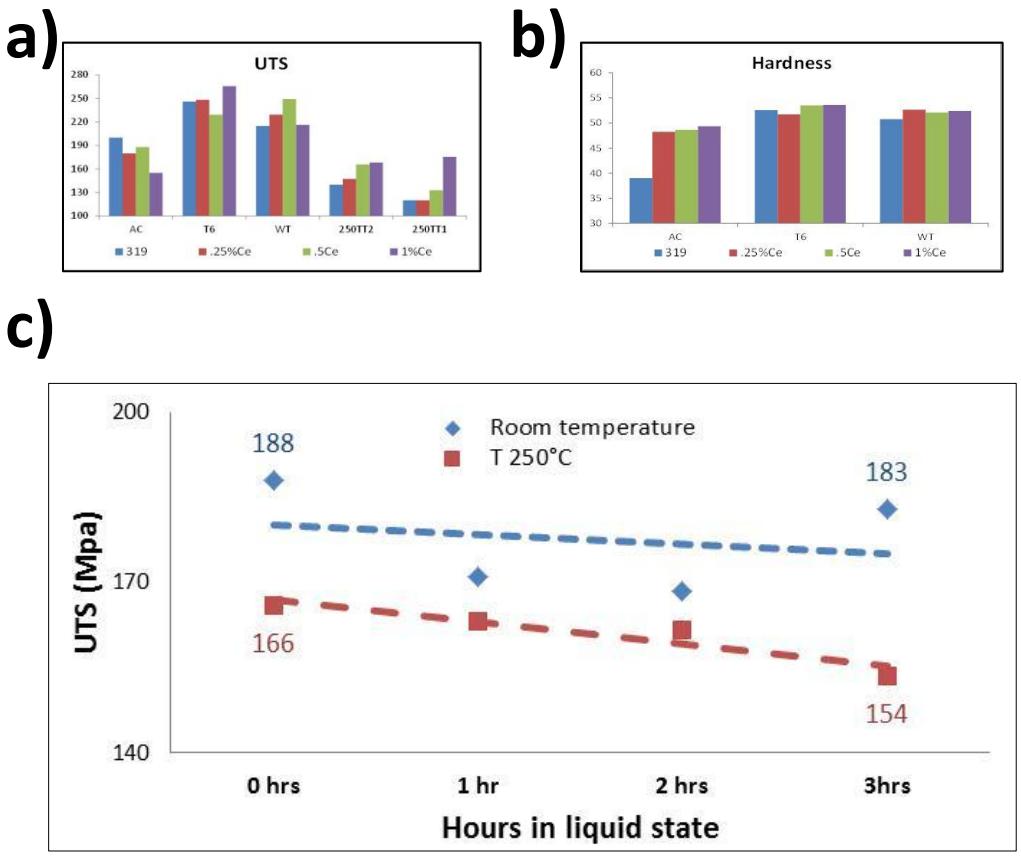

Figure 5. Mechanical properties: a) UTS, b) Rockwell B hardness c) UTS function of time remaining in liquid alloy.

Conclusions

The effect of Cerium and Lanthanum additions on microstructure was evaluated employing aluminum commercial alloy A319. The reduction of eutectic Si phase was the most notorious microstructural change, reducing its precipitate average area functions of Ce/La added. About mechanical properties, the micrometric Ce/La needles like phases that enhance the hardness values on the AC state has an important influence for the θ'

phases, competing for the amount of dissolved copper in the matrix. The time that alloy remained at liquid state is an important degree of freedom to take in account by the continuous decrease in UTS function of time. The results suggest that direct Ce/La additions in casting industrial production processes is applicable to standard industrial casting process extendable to commercial alloys.

Acknowledgements

The authors are grateful with CIMAV-NANOTECH for support provided through Carlos Ornelas, Karla Campos and Rodrigo Dominguez and with Dr. R. Perez-Bustamante and M.C.M. M. Romo-García because useful discussions. JCC is supported by CONACYT PhD scholarship 290674 and 290604.

References

1. F.J. Tavitas-Medrano, J.E. Gruzleski, F.H. Samuel, S. Valtierra, H.W. Doty, Effect of Mg and Sr-modification on the mechanical properties of 319-type aluminum cast alloys subjected to artificial aging, Materials Science and Engineering A, 480, 2008, 356–364.

2. A.T Adorno and R.A.G. Silva, Ageing behavior in the Cu–10 wt.%Al and Cu–10 wt.%Al–4 wt.%Ag alloys, Journal of Alloys and Compounds, 473, 2009, 139–144.

3. P. Muhamed Ashraf and S.M.A. Shibli, Reinforcing aluminium with cerium oxide: A new and effective technique to prevent corrosion in marine environments, Electrochemistry Communications 9 (2007) 443–448.

4. I. Anyanwu, Y. Gokan, A. Suzuki, S. Kamado, Y. Kojima, S. Takeda, T. Ishida, Effect of substituting cerium-rich mischmetal with lanthanum on high temperature properties of die-cast Mg-Zn-Al-Ca-RE alloys, Materials Science and Engineering A 380 (1) (2004) 93–99.

5. O. Sebaie, A. Samuel, F. Samuel, H. Doty, The effects of mischmetal, cooling rate and heat treatment on the eutectic Si particle characteristics of A319.1, A356.2 and A413.1 Al-Si casting alloys, Materials Science and Engineering A 480 (1-2) (2008) 342–355.

6. Mehdi Hosseinifar and Dmitri V. Malakhov, Effect of Ce and La on microstructure and properties of a 6xxx series type aluminum alloy, J Mater Sci (2008) 43:7157–7164.

7. Yu-Chou Tsai, Cheng-Yu Chou, Sheng-Long Lee, Chih-Kuang Lin, Jing-Chie Lin, S.W. Lim, Effect of trace La addition on the microstructures and mechanical properties of A356 (Al–7Si–0.35Mg) aluminum alloys, Journal of Alloys and Compounds, 487, 2009, 157–162.

8. D. Xiao, J. Wang, D. Ding, H. Yang, Effect of rare earth Ce addition on the microstructure and mechanical properties of an Al-Cu-Mg-Ag alloy, Journal of Alloys and Compounds 352 (1-2) (2003) 84–88.

9. E. Rincon, H.F. Lopez, M.M. Cisneros, H. Mancha, M.A. Cisneros, Effect of temperature on the tensile properties of an as-cast aluminum alloy A319, Materials Science and Engineering A, 452–453, 2007, 682–687.

10. A. Mitrasinovic, F.C. Robles Hernandez, M. Djurdjevic, J.H. Sokolowski, On-line prediction of the melt hydrogen and casting porosity level in 319 aluminum alloy using thermal analysis, Materials Science and Engineering A, 428, 2006, 41–46.

11. P. S. Mohanty and J. E. Gruzlesk, Mechanism Of Grain Refinement In Aluminium, Acta metall..tater., Vol. 43, No. 5, pp. 2001 2012, 1995.

12. M. Shabani, M. Emamy, N. Nemati, Effect of grain refinement on the microstructure and tensile properties of thin 319 Al castings, Materials & Design 32 (3) (2011) 1542 – 1547.

13. P.D. Lee, A. Chirazi, R.C. Atwood and W. Wang, Multiscale modelling of solidification microstructures, including microsegregation and microporosity, in an Al–Si–Cu alloy, Materials Science and Engineering A, 365, 2004, 57–65.

14. G. Garcia-Garcia, J. Espinoza-Cuadra, H. Mancha-Molinar, Copper content and cooling rate effects over second phase particles behavior in industrial aluminum-silicon alloy 319, Materials and Design 28 (2) (2007) 428–433.

15. M. Lalpoor, D. Eskin, G. ten Brink, L. Katgerman, Microstructural features of intergranular brittle fracture and cold cracking in high strength aluminum alloys, Materials Science and Engineering: A 527 (7-8) (2010) 1828 – 1834.

16. S. Weakley-Bollin, W. Donlon, W. Donlon, C. Wolverton, J. Allison, J. Jones, Modeling the age-hardening behavior of Al-Si-Cu alloys, Metallurgical and Materials Transactions A 35 (8) (2004) 2407–2418, ISSN 1073-5623.

17. E. Aguirre-De la Torre, R. Pérez-Bustamante, J. Camarillo-Cisneros, C.D. Gomez-Esparza, H.M. Medrano-Prieto, R. Martinez-Sanchez, Mechanical properties of the A356 aluminum alloy modified with La/Ce, Journal Of Rare Earths, Vol. 31, No. 8, Aug. 2013, P. 811.

18. D. Mitlin, J. Morris, J.W., V. Radmilovic, Catalyzed precipitation in Al-Cu-Si, Metallurgical and Materials Transactions A 31 (11) (2000), 2697–2711, ISSN 1073-5623.

19. D. Mitlin, J. Morris, J.W., V. Radmilovic, U. Dahmen, Precipitation and aging in Al-Si-Ge-Cu, Metallurgical and Materials Transactions A, 32 (1) (2001) 197–199, ISSN 1073-5623.

20. D. O. Ovono, I. Guillot, D. Massinon, The microstructure and precipitation kinetics of a cast aluminium alloy, Scripta Materialia 55 (3) (2006) 259 – 262.

21. D. O. Ovono, I. Guillot, D. Massinon, Determination of the activation energy in a cast aluminium alloy by TEM and DSC, Journal of Alloys and Compounds 432 (1-2) (2007) 241 – 246.